Self-organization and Mechanical Properties of Active Filament Bundles

Karsten Kruse[1, 2, 3, *] and Frank Jülicher[1, 2, †]

[1]*Max-Planck-Institut für Physik komplexer Systeme, Nöthnitzer Str. 38, 01187 Dresden, Germany*
[2]*Institut Curie, Physicochimie, UMR CNRS/IC 168, 26 rue d'Ulm, 75248 Paris Cedex 05, France*
[3]*Max-Planck-Institut für Strömungsforschung, Bunsenstr. 10, 37073 Göttingen, Germany*
(Dated: February 1, 2008)

A general framework for the description of active bundles of polar filaments is presented. The activity of the bundle results from mobile cross-links, that induce relative displacements between the aligned filaments. Our generic description is based on momentum conservation within the bundle. By specifying the internal forces, a simple minimal model for the bundle dynamics can be derived, capturing a rich variety of dynamic behaviors. In particular, contracted states as well as solitary and oscillatory waves appear through dynamic instabilities. We present the full bifurcation diagram of this model and study the effects of a dynamic motor distribution on the bundle dynamics. Furthermore, we discuss the mechanical properties of the bundle in the presence of externally applied forces. Our description is motivated by dynamic phenomena in the cytoskeleton and could apply to in vitro experiments as well as to stress-fibers and to self-organization phenomena during cell-locomotion.

I. INTRODUCTION

The cytoskeleton of eucaryotic cells is a complex three dimensional network of protein filaments, most prominently actin filaments and microtubules [1, 2]. Its elastic and viscous properties are essentially defining the mechanical or material properties of living cells. This network resembles in many aspects a polymer solution or a gel. The main difference from usual polymer materials is its intrinsic activity. In fact, the cytoskeleton is constantly remodeled through the polymerization and depolymerization of filaments, as well as through the formation and breakup of cross-links. In addition, the cross-links may be active, leading to further dynamics. Active or mobile cross-links are provided for example by molecular motors which are specialized enzymes which transduce the chemical energy of a fuel to motion along filaments [1, 2, 3, 4]. All these activities are regulated by the cell which is thus able to direct intracellular transport, to separate its chromosomes and to cleave during cell division, to exert forces on the environment, or to move on a substrate.

The study of active polymer systems requires completely new tools and techniques as compared to the well developed analysis of equilibrium properties, that relies on powerful concepts of equilibrium statistical physics. Indeed, such systems are intrinsically far from equilibrium, and the dynamics at equilibrium, that is usually studied in polymer physics [5, 6, 7], is not sufficient for the description of active systems [8]. On the contrary, experimental studies of the cytoskeleton under simplified conditions have revealed its ability to self-organize. Namely, the contraction of filament bundles [9], the formation of asters and vortices [10, 11, 12, 13], as well as

the formation of networks [14] were found in vitro. Using a cell extract, even the formation of bipolar spindles without microtubule organizing centers has been seen [15]. Cell fragments containing only the actin cytoskeleton, but neither the nucleus nor microtubules, can propagate on a substrate [16], where the locomoting state coexists with a stationary spherically symmetric state [17]. In a mixture of actin filaments and myosin molecular motors, active reptation in a polymer solution has been observed [18]. Let us finally mention, that experiments probing mechanical properties of living cells have revealed active responses of the cytoskeleton to external forces, see, e.g., Ref. [19].

First steps towards a theoretical understanding of active polymer systems have mostly aimed at describing pattern-formation. In one-dimensional filament bundles, polarity sorting [20], contraction [21, 22], and propagating waves [23] have been observed. Self-organization has also been seen to induce bending waves and complex motion in axonemes [24, 25]. In higher dimensions, the effects of active cross-links on the formation of orientation patterns in systems of spatially fixed filaments have been studied [26, 27] and the generation of filament currents by active cross-links has been discussed [28]. Furthermore, the viscoelastic response of solutions of semi-flexible polymers and active centers has been studied [29].

Active filament bundles provide very simple examples of active filament networks and can be discussed by a one-dimensional description. Note, however, that in addition to their simplicity, such filament bundles actually occur in animal cells. They are, for example, part of stress fibers which generate contractile forces, and of the contractile ring in dividing cells [2]. In vitro, the contraction of actin bundles in the presence of myosin motors has been observed [9].

Motivated by the dynamics of the cytoskeleton, we develop a general framework based on momentum conservation, to describe the physics of bundles of aligned filaments in the presence of active cross-links. Since actin

*karsten@mpipks-dresden.mpg.de
†julicher@mpipks-dresden.mpg.de

filaments and microtubules are polar as they have two structurally different ends, we consider polar filaments. The cross-links are mobile and considered to be formed by small aggregates of molecular motors of one type. We discuss simple scenarios in order to study dynamic phenomena and mechanical properties of such systems. A minimal model which has been introduced in earlier publications [22, 23] can be derived in our general framework using approximations and simplifications. This model already exhibits many of the phenomena that occur in such systems. However, it neglects changes in the distribution of motors due to the dynamics of the system. This dynamics of the motor distribution can be taken into account within our general framework. Furthermore, we discuss the mechanical properties of active bundles in the presence and absence of external forces.

The outline of our manuscript is as follows. In section II, we introduce the general description for active filament bundles based on momentum balance. Using this formalism we derive dynamic equations for the system. In Section III, we show how the minimal model can be derived from the general equations. We review its properties and extend previous work towards a discussion of the full bifurcation diagram. In Section IV we study the effects of the dynamics of the motor distribution on the filament dynamics. The active mechanical properties of a filament bundle can be derived systematically in the framework introduced in section II. We discuss the bundle mechanics in Section V and study tense states balanced by external forces applied at the ends. The paper concludes with a discussion of our results in Section VI which relates our theoretical framework to experimental situations. The appendices contains a detailed analysis of bifurcations in the minimal model as well as the effects of filament adhesion to a substrate.

II. PHENOMENOLOGICAL DESCRIPTION OF ACTIVE FILAMENT BUNDLES

We introduce a general description for the dynamics of active filament bundles. The bundle is described in one dimension using density profiles of filaments and motors. The dynamics of these densities is governed by currents which are generated by interactions between filaments and motors. Dynamic equations can be derived on the basis of momentum balance. This general procedure can be carried out most conveniently using simplifying assumptions. In particular, we assume a low motor density or low duty ratio of motors such that interactions between filament pairs dominate, a local friction of filaments with the environment and we neglect the possibility of passive cross-linkers. Furthermore, we assume that filament lengths remain fixed, i.e. we neglect polymerization and depolymerization of filaments, and we assume that filaments cannot change their orientation. However, many of the qualitative behaviors displayed by the resulting equations are more general and are also found

in purely phenomenological descriptions which are not based on these simplifying assumptions [30]. The dynamic equations we discuss here represent a mean field theory of filament bundles where fluctuations do not appear explicitly but give rise to diffusive terms.

A. Densities of filaments and motors

The bundle is characterized by the number densities of filaments and of motor complexes projected on the bundle axis, which leads to an effective one-dimensional description. Since filament bending and entanglements can be ignored in the bundle, we describe filaments as rigid rods. Filaments are aligned along the x-axis and we distinguish the two sub-populations of filaments with their plus-end pointing into the positive and negative x-direction, respectively. These populations are described by the densities c^+ and c^-, such that, e.g., $c^+(x)dx$ gives the number of filaments with their plus-end in the positive x-direction and their center located in the interval $[x, x + dx]$. We assume, that motors are small compared to the filament length and will be treated as point-like in our description. The number density of motors is denoted by m.

The filament and motor densities satisfy the conservation laws

$$\partial_t c^+ = D\partial_x^2 c^+ - \partial_x J^+ \tag{1}$$
$$\partial_t c^- = D\partial_x^2 c^- - \partial_x J^- \tag{2}$$
$$\partial_t m = D_m\partial_x^2 m - \partial_x J \tag{3}$$

Here, the currents $J^\pm$ and J are generated by the active interaction between motors and filaments. The densities c^+ and c^- are conserved separately since we do not allow filaments to change their orientation. Fluctuations in the system give rise to diffusive terms with diffusion coefficients D and D_m of filaments and motors. While the diffusion of motors could be expected to result from thermal fluctuations, the diffusion of filaments is generated effectively by fluctuations of the forces induced by motor-filament interactions. For long filaments, the contribution of thermal fluctuations to the diffusion coefficient D is negligible. We return to this point in Sect. VI.

B. Momentum balance

In the absence of external forces, the total momentum is conserved in the filament bundle. Forces acting within the bundle lead to an exchange of momentum with the environment or between filaments. Since filaments are treated as rigid, extended objects with momentum distributed along the full length of the filament, we introduce the momentum densities $\pi^\pm(x, y)$. These densities represent the momentum at position y carried by all plus- or minus-filaments, respectively, with their centers

located at position x. The momentum balance can then be expressed as

$$\partial_t \pi^+(x,y) + \partial_y \sigma^+(x,y) - f_{\text{int}}^+(x,y) = f_{\text{fl}}^+(x,y) + f_{\text{m}}^+(x,y) + f_{\text{ext}}^+(x,y) \tag{4}$$

$$\partial_t \pi^-(x,y) + \partial_y \sigma^-(x,y) - f_{\text{int}}^-(x,y) = f_{\text{fl}}^-(x,y) + f_{\text{m}}^-(x,y) + f_{\text{ext}}^-(x,y) \tag{5}$$

Here, momentum flux along filaments centered at x is given by the tensions $\sigma^\pm(x,y)$. Momentum exchange between filaments is nonlocal and described by the internal force densities $f_{\text{int}}^\pm(x,y)$, which include all active filament interactions via motors. The force densities $f_{\text{fl}}^\pm(x,y)$, $f_{\text{m}}^\pm(x,y)$, and $f_{\text{ext}}^\pm(x,y)$ are source and sink terms, describing momentum exchange with the environment. They result from friction with the fluid (f_{fl}), from motors moving along a single filament (f_{m}), and from external forces (f_{ext}). Here, x refers to filaments with center at position x, while y denotes a position in space, where a force is acting and momentum is exchanged. Momentum conservation in the absence of external forces requires, that

$$\int dx \left[f_{\text{int}}^+(x,y) + f_{\text{int}}^-(x,y) \right] = 0 \quad . \tag{6}$$

This implies, that any force generated by active cross-links on a filament is balanced by an opposite force acting on other filaments, i.e., internal forces at a point y are balanced when integrated over all filaments. Therefore, total momentum $\Pi = \int dx\, dy (\pi^+ + \pi^-)$ changes according to (ignoring boundary terms):

$$\frac{d}{dt}\Pi = \int dx\, dy \left[f_{\text{ext}}^+(x,y) + f_{\text{ext}}^-(x,y) + f_{\text{fl}}^+(x,y) + f_{\text{fl}}^-(x,y) + f_{\text{m}}^+(x,y) + f_{\text{m}}^-(x,y) \right] \tag{7}$$

Inertial terms are negligible in a slowly moving bundle, such that we can set $\partial_t \pi^\pm = 0$. Equations (4) and (5) then express a balance of forces.

In the most simple case where friction is local, we can write for the density of friction forces

$$f_{\text{fl}}^\pm(x,y) = \eta J^\pm(x) R(x-y) \tag{8}$$

Here, η is a friction coefficient per unit length and $R(x)$ is a function characterizing the distribution of energy dissipation along moving filaments. If all filaments are of the same length ℓ, a simple choice is $R(x) = 1$ for $|x| < \ell/2$ and $R(x) = 0$ otherwise. However, the function $R(x)$ can also account for situations with a distribution of filament lengths. Then, $R(x)$ is related to the probability, that a given filament is longer than $2|x|$.

The forces exerted by motors moving along a single filament are linear in the filament and motor densities,

$$f_{\text{m}}^\pm(x,y) = \mp \eta_{\text{m}} \Gamma m(y) c^\pm(x) R(x-y) \quad , \tag{9}$$

where η_{m} is the friction coefficient corresponding to single motors and the coefficient Γ characterizes the binding to and motion on filaments of individual motors

C. Currents of filaments and motors

While the internal forces are balanced at a point y when integrated over all filaments, the total force $\int dy f_{\text{int}}^\pm(x,y)$ acting on filaments centered at a given position x does not vanish in general. Integration of Eqs. (4) and (5) with respect to y reveals that this force is balanced by friction forces:

$$\eta \ell J^\pm(x) = - \int dy \left[f_{\text{int}}^\pm(x,y) + f_{\text{m}}^\pm(x,y) \right] \tag{10}$$

where $\ell = \int dx R(x)$ is the average filament length and where we have assumed $f_{\text{ext}} = 0$. Since friction of motors is small as compared to filament friction, $\eta_{\text{m}} \ll \eta \ell$, the contribution of $f_{\text{m}}^\pm$ can be neglected in most practical cases, in particular, for low motor densities. In the following, we therefore set $\eta_{\text{m}} = 0$.

In order to write explicit expressions for the currents, we need a model for the internal forces in the bundle. We consider the case when clusters of three or more cross-linked filaments form rarely enough, such that their contribution to the internal forces can be neglected. This holds in the case of a low motor density or for motors with a low duty ratio, which is the fraction of time a motor spends attached to a filament [31]. If interactions between filament pairs dominate, we can split the internal forces into those between filaments of the same and

those of opposite orientation. We write

$$f_{\text{int}}^{+} = f_{\text{int}}^{++} + f_{\text{int}}^{+-} \tag{11}$$

and analogously for f_{int}^{-}. A motor may link two filaments

and thus exert forces of opposite sign on each of them, whenever they overlap. Assuming that the probability for two filaments to interact increases quadratically with filament density, we write

$$f_{\text{int}}^{\pm\pm}(x,y) = \int dz\, c^{\pm}(x)c^{\pm}(z)\, R(y-x)R(y-z)\, m(y)F^{\pm\pm}(z-x,y-x) \tag{12}$$

and corresponding expressions for $f_{\text{int}}^{\pm\mp}$. Here, $F^{++}(\xi,\zeta)$ is the average force acting on plus-filaments at a distance ζ from the center exerted by motors, that interact with other minus-filaments located at a distance ξ from the first, see Fig. 1. The essential feature of motor-filament interactions is that the direction of the force applied by a motor on a filament is uniquely determined by the orientation of the filament [32]. The product $R(y-x)R(y-z)$ gives the probability, that a filament at x has an overlap at y with a filament at z. Here, the position of a filament is given by the position of the filament's center. Analogous expressions hold for the internal forces between minus-filaments as well as between filaments of opposite orientation.

The forces $F^{\pm\pm}$ and $F^{\pm\mp}$ obey the following symmetry relations. Momentum balance demands that under an exchange of filaments, the force changes sign:

$$F^{\pm\pm}(\xi,\zeta) = -F^{\pm\pm}(-\xi,\zeta-\xi) \tag{13}$$
$$F^{\pm\mp}(\xi,\zeta) = -F^{\mp\pm}(-\xi,\zeta-\xi) \tag{14}$$

see Fig. 1. Using relation (12), the internal forces satisfying the above equations verify Eq. (6), which assures momentum conservation. Space inversion symmetry re-

quires

$$F^{++}(\xi,\zeta) = -F^{--}(-\xi,-\zeta) \tag{15}$$
$$F^{+-}(\xi,\zeta) = -F^{-+}(-\xi,-\zeta) \tag{16}$$

Momentum conservation also determines the non-diffusive motor current J with

$$-\eta_m J(y) = \int dx [f_{\text{m}}^{+}(x,y) + f_{\text{m}}^{-}(x,y)] \tag{17}$$

Here the forces of individually bound motors are defined in Eq. (9).

The continuity Eqs. (1)-(3) for the densities together with the defining Eqs. (10) and (12) of filament currents and Eq. (17) for the motor currents provide the full dynamic equations of active filament bundles. The functions $F^{\pm\pm}$ depend on the details of the motor-filament interactions and could be modified by further proteins bound to the filaments. However, the large scale behaviors of the system do not depend on the detailed form of these functions. In the following sections, we will therefore make simple choices which obey the symmetry relations discussed above.

III. THE MINIMAL MODEL

The minimal model has been introduced in Ref. [22] as a simple model for filament dynamics. It can be obtained from the general equations derived in the previous section by choosing $R(x) = 1$ for $|x| < \ell/2$ and $R(x) = 0$ otherwise. The forces $F^{\pm\pm}$ are chosen to behave as

$$F^{\pm\pm}(\xi,\zeta) \sim \text{sgn}(\xi)$$
$$F^{\pm\mp}(\xi,\zeta) \sim \mp 1 \quad, \tag{18}$$

where $\text{sgn}(\xi) = 1$ for $\xi > 0$ and -1 otherwise, which represents the simplest choice compatible with the symmetry requirements. Furthermore, we assume in the minimal model that the motor distribution is homogeneous and its dynamics can be neglected.

The resulting dynamical equations are most conveniently expressed in dimensionless form. We define $\tilde{x} = x/\ell$ and measure lengths in units of the filament length

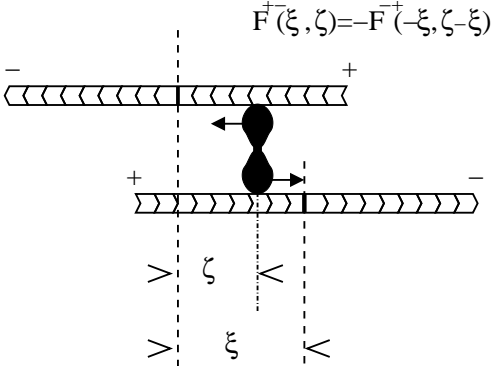$$\vec{F}^{+-}(\xi,\zeta) = -\vec{F}^{-+}(-\xi,\zeta-\xi)$$

FIG. 1: Schematic representation of the forces exerted by an active cross-link on two filaments of opposite orientation. The centers of the filaments are indicated by the dashed lines, whereas the dotted-dashed line marks the position of the active cross-link. The arrows indicate the direction of the forces applied by motors on the filaments.

ℓ, and a dimensionless time variable $\tilde{t} = tD/\ell^2$. Furthermore, we introduce dimensionless densities $\tilde{c} = c\ell$. Suppressing the tildes, the dynamic equations of the minimal model can be written as

$$\partial_t c^+(x) = \partial_x^2 c^+(x) - \alpha \partial_x \int_0^1 d\xi \, [c^+(x+\xi) - c^+(x-\xi)]c^+(x)$$

$$+ \beta \partial_x \int_{-1}^1 d\xi \, c^-(x+\xi)c^+(x) \tag{19}$$

$$\partial_t c^-(x) = \partial_x^2 c^-(x) - \alpha \partial_x \int_0^1 d\xi \, [c^-(x+\xi) - c^-(x-\xi)]c^-(x)$$

$$- \beta \partial_x \int_{-1}^1 d\xi \, c^+(x+\xi)c^-(x) \quad . \tag{20}$$

where α and β are dimensionless coupling constants characterizing the strength of the motor forces defined in Eqs. (18). It follows from the dynamical equations, that the homogeneous state $c^\pm(x) = c_0^\pm = const.$ is a stationary solution for all values of the parameters.

A. Oriented bundles - Contraction

If all filaments are of the same orientation, one is left with a single equation

$$\partial_t c(x) = \partial_x^2 c(x) - \alpha \partial_x \int_0^1 d\xi \, [c(x+\xi) - c(x-\xi)] \, c(x) \quad . \tag{21}$$

Here, c represents either c^+ or c^-, depending on the orientation of the filaments. This nonlinear integro-differential equation is the most simple description of the active dynamics of a filament bundle. Many of the basic physical principles underlying self-organization of filament bundles can already be discussed using this equation.

1. Linear stability

We consider a system of length L with periodic boundary conditions and study the stability of the homogeneous state with respect to small perturbations. Periodic boundary conditions imply that the bundle forms a ring. Such rings appear, e.g., in eucaryotic cells, in the late stages of cell division. We represent the filament density by a Fourier expansion

$$c(x) = \sum_k c_k e^{ikx} \quad , \tag{22}$$

with $k = 2\pi n/L$, $n = 0, \pm 1, \ldots$ and where $c_{-k} = c_k^*$. Up to first order in the Fourier components c_k, the dynamics

(21) reads

$$\frac{d}{dt}c_k = -\left(k^2 - 2\alpha c_0\left(1 - \cos k\right)\right)c_k \tag{23}$$

$$\equiv \lambda(k)c_k \quad , \tag{24}$$

for all k. This relation implies that for $\alpha c_0 \leq k^2/2(1 - \cos k)$ the mode c_k decays in time, because then $\lambda(k) \leq 0$. It follows that the most unstable mode is the one corresponding to the smallest non-zero wave number $k = 2\pi n/L$ with $n = 1$. This can be demonstrated using $(\frac{2\pi}{L})^2/2(1 - \cos\frac{2\pi}{L}) \leq (\frac{2\pi n}{L})^2/2(1 - \cos\frac{2\pi n}{L})$ for all $n > 1$ which can be verified by induction using the equivalent condition $n^2 - n^2\cos(2\pi/L) - 1 + \cos(2\pi n/L) \geq 0$. Therefore, the homogeneous state is linearly stable as long as $\alpha \leq \alpha_c$, where the critical value α_c is determined by $\lambda(2\pi/L) = 0$. Explicitly,

$$\alpha_c = \frac{2\pi^2}{c_0 L^2(1 - \cos(2\pi/L))} \quad . \tag{25}$$

The critical value α_c is positive and decreases with increasing c_0 and L (for $L \geq 1$). Note, that for bundle sizes $L \geq 1$, we have $0 < \alpha_c < \infty$.

2. Contracted states

If the homogeneous state is unstable, the system evolves to an inhomogeneous steady state. We can calculate this state by numerically solving the dynamic equations or, in the vicinity of the bifurcation, using a systematic expansion in Fourier modes. To third order in c_1 the equation for the steady state $\partial_t c = 0$ reads

$$F(\alpha)c_1 - G(\alpha)|c_1|^2 c_1 = 0 \quad , \tag{26}$$

with $F(\alpha) = \lambda(2\pi/L)$ and $G(\alpha)$ given by Eqs. (B6) and (B7), see Appendix B. Note, that $F(\alpha_c) = 0$. Expanding F and G at $\alpha = \alpha_c$, we find expressions for the Fourier amplitudes c_1 and c_2, given by Eqs. (B8) and (B9). This
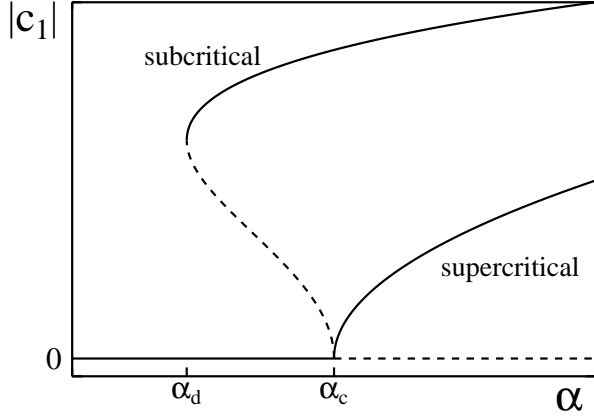
FIG. 2: Schematic representation of the amplitude $|c_1|$ of the first spatial Fourier-component of stationary states as a function of the coupling strength between equally oriented filaments α. Presented are the cases of a super- and of a subcritical bifurcation. Solid lines represent stable, dashed lines unstable solutions. In both cases, the homogeneous state is stable for $\alpha < \alpha_c$ and unstable otherwise. In the supercritical case, i.e., if $F/G > 0$ for $\alpha > \alpha_c$, the bifurcating solution exists for $\alpha > \alpha_c$ and is stable, while in the other case it exists for $\alpha < \alpha_c$ and is unstable. In the latter case, one usually finds inhomogeneous solutions coexisting with the homogeneous state in an interval $[\alpha_d, \alpha_c]$.
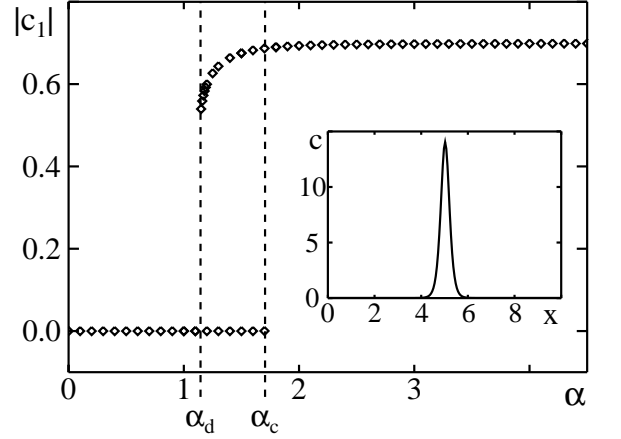

FIG. 3: The amplitude of the first Fourier-component of stable stationary solutions of the minimal model for an oriented bundle as a function of the interaction strength α. The average filament concentration is $c_0 = 0.7$ and system size $L = 10$. The inset presents the non-homogeneous stationary solution for $\alpha = 1.5$. The scenario shown corresponds to a subcritical bifurcation, see Fig. 2.

For large α we find numerically, that transient states consisting of several contracted packets can occur, which however decay for long times to a steady state with one maximum. Their lifetime increases with increasing α.

3. Contraction dynamics

The contraction of the bundle is most conveniently discussed in an infinite system using the variance of the filament distribution

$$\sigma^2 = \frac{1}{N} \int_{-\infty}^{\infty} dx \, x^2 c(x) \quad , \tag{27}$$

where $N = \int_{-\infty}^{\infty} dx \, c(x)$ is the total number of filaments, as a measure of bundle contraction. Since the center of mass of the distribution is immobile due to momentum conservation, we have chosen without loss of generality $\langle x \rangle = \int_{-\infty}^{\infty} dx \, xc(x) = 0$. The variance changes in time as

solution represents a localized distribution of filaments, i.e., a contracted bundle.

It follows from Eq. (26), that this contracted steady state exists if $F(\alpha)/G(\alpha) > 0$. Depending on whether the ratio F/G is positive for $\alpha > \alpha_c$ or for $\alpha < \alpha_c$, the bifurcation is supercritical and subcritical, respectively, see Fig. 2. From Eq. (B8) one deduces that the bifurcation is supercritical for system sizes falling within particular intervals for which $4/(4n-1) < L < 4/(4n-3)$, $n = 1, 2, \ldots$.

Figure 3 presents numerical solutions of the dynamical equations using an Euler-algorithm with spatial discretization $\Delta = 0.1$. Displayed is the modulus of the first Fourier-component $|c_1|$ of the attractors as a function of α for a system of length $L = 10$. A region of coexistence extends from $\alpha = \alpha_d$ up to α_c, where the homogeneous state becomes unstable.

$$
\begin{aligned}
\frac{d}{dt}\sigma^2 &= \frac{1}{N} \int_{-\infty}^{\infty} dx \, x^2 \partial_t c(x,t) \\
&= \frac{2}{N} \int_{-\infty}^{\infty} dx \, c(x,t) + \frac{2}{N} \int_0^1 d\xi \left[\int_{-\infty}^{\infty} dx \, xc(x+\xi)c(x) - \int_{-\infty}^{\infty} dx \, xc(x-\xi)c(x) \right] \\
&= 2 - \frac{2}{N}\alpha \int_0^1 d\xi \, \xi \int_{-\infty}^{\infty} dx \, c(x+\xi)c(x) \quad .
\end{aligned}
\tag{28}
$$

The final expression reveals two opposing effects. The positive constant describes the spreading of the bundle due to fluctuations while the second term takes into account the effect of the active interactions. The interaction between parallel filaments tends to contract the bundle. Note, that distributions for which $d\sigma^2/dt = 0$ do not necessarily correspond to stationary solutions of the dynamics (21).

B. Bundles of mixed orientation - Solitary waves

1. Linear stability

The linearization of Eqs. (19) and (20) around the homogeneous state $c^\pm(x) = c_0^\pm = const$ reads in Fourier-representation

$$\frac{d}{dt}\begin{pmatrix} c_k^+ \\ c_k^- \end{pmatrix} = \begin{pmatrix} \Lambda^{++} & \Lambda^{+-} \\ \Lambda^{-+} & \Lambda^{--} \end{pmatrix}\begin{pmatrix} c_k^+ \\ c_k^- \end{pmatrix} \quad , \quad (29)$$

where the elements of the matrix $\Lambda(k)$ are given by

$$\Lambda^{\pm\pm}(k) = -k^2 - 2\alpha(\cos(k) - 1)c_0^\pm \pm 2i\beta k c_0^\mp$$
$$\Lambda^{\pm\mp}(k) = \pm 2i\beta \sin(k)c_0^\pm \quad . \quad (30)$$

For a system of length L with periodic boundary conditions, the wave numbers are $k = 2\pi n/L$ with $n = 0, 1, \ldots$. In presence of the coupling between the filaments of opposite orientation, the matrix Λ is not diagonal. The stability of the modes is determined by the larger of the real parts $\lambda(k)$ of the complex eigenvalues of this matrix which are given in App. A.

We find again that the mode with the smallest wave number $k = 2\pi/L$ is most unstable and there exists a critical value α_c where the homogeneous state becomes linearly unstable. Furthermore, $\alpha_c \geq 0$, independently of the values of the other parameters, see App. A. The critical value

$$\alpha_c \equiv \frac{1}{c}g\left(\beta, \frac{\delta c}{c}, L\right), \quad (31)$$

is a function of the remaining parameters, where $c = c_0^+ + c_0^-$ and $\delta c = c_0^+ - c_0^-$. Here, g is a dimensionless scaling function. In some limiting cases, explicit expressions for α_c can be obtained. For example, for $\delta c = 0$ one finds $g = 4\pi^2/L^2[1 - \cos(2\pi/L)]$ and in the limit $L \to \infty$ $g = 1$ if $\beta \neq 0$, whereas $g = 2/(1 + |\delta c|/c)$ for $\beta = 0$, see Eq. (25). These expressions reflect some interesting properties of α_c, e.g., it decreases monotonically with $|\delta c|/c$, L, and $|\beta|$ [22].

2. Solitary waves

For $\beta \neq 0$, the eigenvalues of $\Lambda(k)$ are complex and the homogeneous state loses stability through a Hopf-bifurcation, leading to solutions that oscillate in time.

We find that at the bifurcation a solitary wave of the form $c^\pm(x, t) = u^\pm(x - vt)$ occurs. From momentum conservation, it follows that the total filament current

$$I = \int dx \, (J^+ + J^-) \quad (32)$$

vanishes. This implies that the propagating filament pattern is not accompanied by a net filament transport. However, as soon as filament adhesion to a substrate is introduced, the total filament current associated with a solitary wave no longer vanishes and self-organized filament transport occurs [23], see App. C.

For weak interactions between filaments of opposite orientation, $|\beta| \ll 1$, solitary waves can be understood intuitively. They emerge from the interaction of a contracted distribution of filaments of one orientation with a homogeneous distribution of filaments of opposite orientation. This picture suggests a systematic procedure for determining solitary waves. Writing $c^\pm(x, t) = u^\pm(x - vt)$, we can expand $u^\pm(x)$ in powers of β. For $\beta = 0$, we start from steady states as discussed above, which we denote as $c^\pm(x, t) = u_0^\pm(x)$. Solitary waves are obtained by assuming that, e.g., u_0^+ is a contracted steady state, while u_0^- is homogeneous. We can now write

$$u^\pm(x) = u_0^\pm(x) + u_1^\pm(x)\beta + u_2^\pm\beta^2 + \ldots \quad (33)$$
$$v = v_1\beta + v_3\beta^3 + \ldots \quad (34)$$

The even terms in the expansion for v vanish by symmetry. To lowest order, we obtain

$$v_1 = 2c_0^- \quad (35)$$
$$u_1^+ = 0 \quad (36)$$
$$u_{1,k}^- = -\frac{2i \sin k \, c_0^- u_{0,k}^+}{k^2 - 2\alpha(1 - \cos k)c_0^-} \quad \text{for } k \neq 0. \quad (37)$$

This result agrees with numerical solutions of Eqs. (19) and (20), see Ref. [23]. For any β, solitary wave solutions can be obtained near the instability via a systematic expansion in Fourier modes, see App. B 2.

3. Bifurcation diagrams

The arguments of the previous subsection suggest a general scenario of bifurcations as the interaction strength α is increased. This scenario emerges from the situation with $\beta = 0$, where the two subpopulations evolve independently, if β becomes nonzero. For small α the homogeneous state is stable. At the critical value α_c, corresponding to the instability of one filament population at $\beta = 0$, a solitary wave occurs. Furthermore, a second bifurcation where the solitary wave loses its stability occurs at α_c'. This second bifurcation is related to the point where the second filament population becomes unstable for $\beta = 0$. This bifurcation leads to an oscillating wave solution which consists of two oscillating distributions, which periodically penetrate each other. An
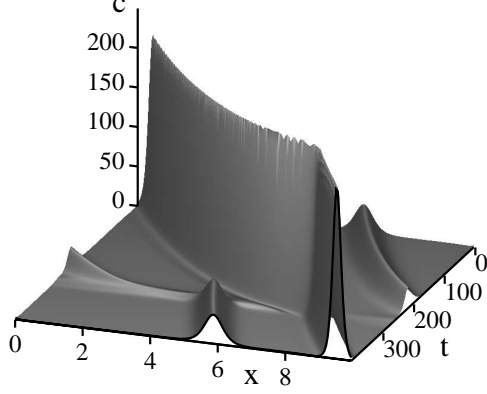
FIG. 4: Total filament concentration $c = c^+ + c^-$ as a function of position x and time t for An oscillating wave solution of the minimal model for coupling parameters $\alpha = 2.5$ and $\beta = 1.$, average filament densities $c_0^+ = 0.7$ and $c_0^- = 0.3$, and system size $L = 10$.

example of such an oscillating wave is shown in Fig. 4. It is characterized by propagating filament profiles which oscillate.

These arguments allow us to derive, the full bifurcation scenario for small values of β. For $\alpha_d < \alpha < \alpha_c$ homogeneous distributions and solitary waves coexist. Similarly, we find a coexistence of oscillating and solitary waves for $\alpha_d' < \alpha < \alpha_c'$. Depending on the ratio of plus- and minus-filament numbers, c_0^+/c_0^-, we find different bifurcation scenarios, see Fig. 5. For large ratios, $\alpha_c < \alpha_d'$ and the coexistence regions are separated. In the second case of similar filament numbers shown in Fig. 5, $\alpha_d' < \alpha_c$ and multiple coexistence occurs, in particular a coexistence of two different solitary waves indicated as S_1 and S_2. These waves move into opposite directions. For the special case $c_0^+ = c_0^-$, the system is symmetric under $x \to -x$ and the coexisting waves S_1 and S_2 occur via spontaneous symmetry breaking.

For three different values of β, numerically obtained bifurcation diagrams are displayed in Fig. 5. Shown is $\langle|c_1^+| + |c_1^-|\rangle$, i.e., the time-averaged sum of the amplitudes of the first spatial Fourier components of both distributions as a function of α. For $\beta = 0.001$ the diagram follows closely the curves shown in the bottom panel corresponding to the limit of small β. As β is increased, the coexistence regions shrink and the solitary wave S_2 disappears. The bifurcation from solitary waves to oscillating waves becomes supercritical for large β.

IV. DYNAMIC MOTOR DISTRIBUTIONS

Motors are actively transported along filaments which in general leads to dynamic changes in the motor distribution [27, 33]. In the previous section, we have assumed
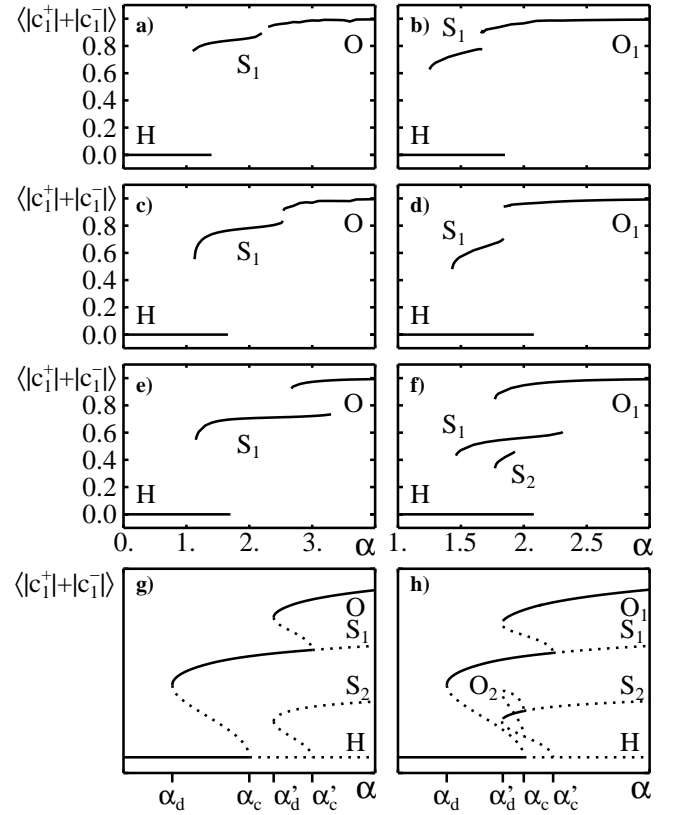

FIG. 5: Asymptotic solutions of the minimal model represented by the time-averaged total amplitude $|c_1^+| + |c_1^-|$ of the first spatial Fourier-components as a function of the interaction strength α for different values of the interaction strength β. The homogenous state is indicated by H, solitary waves by S, and oscillatory waves by O. (a)-(f) have been obtained by numerical integration of the minimal model, where $\beta = 0.1$ for (a) and (b), $\beta = 0.01$ for (c) and (d), and $\beta = 0.001$ for (e) and (f). (a), (c), (e) are for $c_0^+ = 0.7$ and $c_0^- = 0.3$, while (b), (d), (f) are for $c_0^+ = 0.55$ and $c_0^- = 0.45$. In all cases $L = 10$. (g) and (h) give a schematic representation valid for $|\beta| \ll 1$ derived from the bifurcation diagram for $\beta = 0$ as explained in the text. Dashed lines indicate unstable solutions.

that the motor distribution remains homogeneous, which implies that motors diffuse infinitely fast. We will now discuss the effects of the dynamics of the motor distribution using the same choices for the motor forces as given by Eqs. (18) and we assume that filaments are of the same length ℓ.

A. Dynamical equations

The dynamic equations, including the dynamics of the motor density, have been derived in section II. As in the last section, we use dimensionless space and time coordinates, $\tilde{x} = x/\ell$ and $\tilde{t} = tD/\ell^2$ as well as dimensionless densities $\tilde{c}^\pm$. We introduce a dimensionless motor density $\tilde{m} = m/m_0$, where $m_0 = \frac{1}{L}\int_0^L dx\, m(x)$ and L is the

system size. Furthermore, we define the dimensionless parameters $\tilde{\Gamma} = \Gamma \ell / D$, and $\tilde{D}_\mathrm{m} = D_\mathrm{m}/D$. Suppressing the tildes we obtain

$$\partial_t c^\pm = \partial_x^2 c^\pm - \partial_x J^{\pm\pm} - \partial_x J^{\pm\mp} \tag{38}$$

$$\partial_t m = D_\mathrm{m} \partial_x^2 m - \partial_x J \tag{39}$$

with

$$J^{\pm\pm}(x) = A \int_{-1}^1 d\xi \, \mathrm{sgn}(\xi) \, M(x,\xi) c^\pm(x+\xi) c^\pm(x) \tag{40}$$

$$J^{\pm\mp}(x) = \mp B \int_{-1}^1 d\xi \, M(x,\xi) c^\mp(x+\xi) c^\pm(x) \tag{41}$$

$$J(x) = \Gamma \int_{-\frac{1}{2}}^{\frac{1}{2}} d\xi \left[c^+(x+\xi) - c^-(x+\xi) \right] m(x) \tag{42}$$

Here M is the number of motors present in the overlap

region of two filaments with $M(x,\xi) = \int_{x-\frac{1}{2}+\xi}^{x+\frac{1}{2}} d\zeta \, m(\zeta)$ for $\xi > 0$ and $M(x,\xi) = \int_{x-\frac{1}{2}}^{x+\frac{1}{2}+\xi} d\zeta \, m(\zeta)$ for $\xi < 0$. Furthermore, the dimensionless coupling constants A and B are related to the parameters α and β of the minimal model and describe effective interactions of a motor with a filament pair.

B. Oriented bundles

We consider again a system of length L with periodic boundary conditions and all filaments of the same orientation characterized by the density $c(x)$. The dynamic equations linearized at the homogeneous state with $c(x) = c_0$ and $m(x) = m_0 = 1$ read in Fourier representation

$$\frac{d}{dt} \begin{pmatrix} c_k \\ m_k \end{pmatrix} = \begin{pmatrix} -k^2 + 2A(1 - \frac{\sin k}{k})c_0 & -2A(\cos \frac{k}{2} - \frac{2}{k} \sin \frac{k}{2})c_0^2 \\ -2i\Gamma \sin \frac{k}{2} & -D_\mathrm{m} k^2 - i\Gamma k c_0 \end{pmatrix} \begin{pmatrix} c_k \\ m_k \end{pmatrix} \quad , \tag{43}$$

where $k = 2\pi n/L$, with n being integer. For $\Gamma/D_\mathrm{m} \to 0$, we recover the minimal model discussed in the previous section. In contrast to the minimal model, the eigenvalues of (43) are complex if $\Gamma \neq 0$. The homogeneous state thus loses stability through a Hopf-bifurcation, where the most unstable mode occurs at a characteristic wave-number k_0. As a consequence, for larger system sizes, solitary waves with multiple maxima appear, see Fig. IV B. Furthermore, oscillatory waves which can coexist with solitary waves have been found, in contrast to oriented bundles in the minimal model.
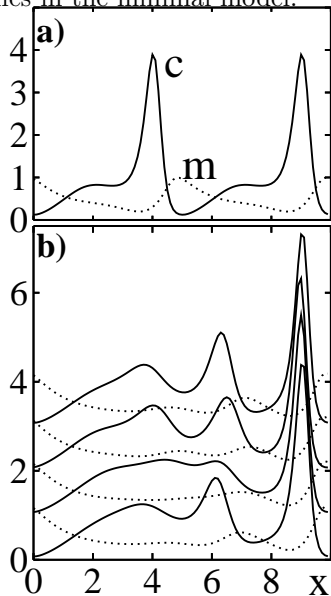
C. Bundles of mixed orientation

In the case of mixed bundles, the linearized equations read in Fourier representation

$$\frac{d}{dt} \begin{pmatrix} c_k^+ \\ c_k^- \\ m_k \end{pmatrix} = \begin{pmatrix} \Lambda^{++} & \Lambda^{+-} & \Lambda^{+\mathrm{m}} \\ \Lambda^{-+} & \Lambda^{--} & \Lambda^{-\mathrm{m}} \\ \Lambda^{\mathrm{m}+} & \Lambda^{\mathrm{m}-} & \Lambda^{\mathrm{mm}} \end{pmatrix} \begin{pmatrix} c_k^+ \\ c_k^- \\ m_k \end{pmatrix}, \tag{44}$$

where the elements of the matrix $\Lambda(k)$ are

$$\Lambda^{\pm\pm}(k) = -k^2 + 2A(1 - \frac{\sin k}{k})c_0^\pm \pm iBk c_0^\mp$$

$$\Lambda^{\pm\mp}(k) = \pm 2iB \frac{1 - \cos k}{k} c_0^\pm$$

$$\Lambda^{\pm\mathrm{m}}(k) = -2A(\cos \frac{k}{2} - \frac{2}{k} \sin \frac{k}{2})c_0^{\pm 2} \pm 2iB \sin \frac{k}{2} c_0^+ c_0^-$$

$$\Lambda^{\mathrm{m}\pm}(k) = \mp 2i\Gamma \sin \frac{k}{2}$$

$$\Lambda^{\mathrm{mm}}(k) = -D_\mathrm{m} k^2 - i\Gamma k(c_0^+ - c_0^-)$$

FIG. 6: Examples of asymptotic solutions for an oriented bundle, where the dynamics of the motor distribution has been taken into account. (a) shows a solitary wave with a spatial period of half the system size, (b) an oscillatory wave. The solid lines represent the filament distributions, the dashed lines the motor distributions. (b) distributions at four different times are shown. They have been shifted in the y-direction for better visibility and in the x-direction such that the positions of the maxima coincide. The two solutions in (a) and (b) exist for the same parameters, which are $A = 1.5$, $\Gamma = 1.5$, $D_\mathrm{m} = 1.$, $c_0 = 1.$, $m_0 = 0.5$, and $L = 10$.
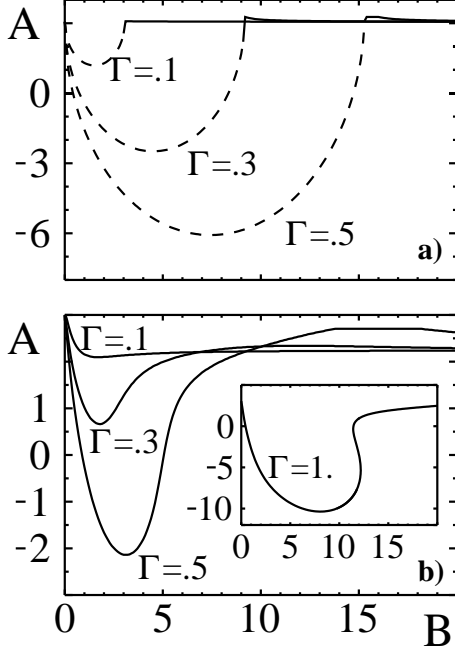
FIG. 7: Regions of stability of the homogeneous state for a filament-bundle with dynamic motor distribution. A and B characterize the coupling of a filament pair via a motor, where the homogeneous state is stable below the lines shown. (a) is for the symmetric case $c_0^+ = c_0^- = 1$, (b) for $c_0^+ = 1$ and $c_0^- = 0.5$. In both cases, $L = 10$ and $D_{\mathrm{m}} = 1$. Solid lines indicate oscillatory instabilities, dashed lines static instabilities. The inset presents a case where increasing A can re-stabilize the homogeneous state.

Fig. 7 displays the line in the (A, B)-plane limiting the region of stability of the homogeneous state for different values of Γ. In contrast to the minimal model, it depends non-monotonically on B. This implies that upon increasing B the homogeneous state can be re-stabilized. For large enough Γ we even find reentrant behavior with respect to A, i.e., increasing A can re-stabilize the homogeneous state, see Fig. 7. Furthermore, the figure shows that the critical values of A can become negative. This implies that the homogeneous state can become unstable even if interactions between parallel filaments are absent i.e. $A = 0$. Another interesting observation is that for $c_0^+ = c_0^-$ the homogeneous state becomes unstable with respect to stationary inhomogeneous states in certain parameter ranges of B. These inhomogeneous stationary states represent a new type of solution as compared to the minimal model of bundles of mixed orientation.

Dynamic solutions to this model can be studied numerically. We find the three types of solutions discussed before namely homogeneous states, solitary waves, and oscillatory waves. In addition we obtain the inhomogeneous stationary state mentioned above which is a one-dimensional analog of asters in higher dimensions and consist of localized distributions of motors and filaments,
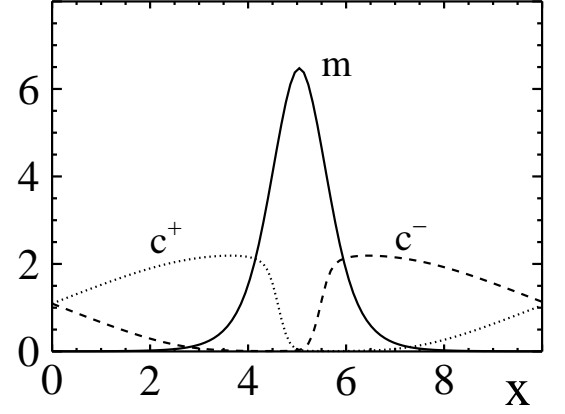

FIG. 8: Inhomogeneous steady state of a symmetric system with $c_0^+ = c_0^-$ where the dynamics of the motor distribution m has been taken into account. The filament distributions are represented by dotted and dashed lines for c^+ and c^-, respectively, the full line represents the motor density m. The parameters are $c_0^+ = c_0^- = 1$, $B = \Gamma = D_{\mathrm{m}} = 1$, and $L = 10$.

see Fig. 8. In contrast to the minimal model, solitary waves can exist even in the absence of interactions between filaments of opposite orientation ($B = 0$) and stationary inhomogeneous states can exist for $B \neq 0$. Interestingly, the direction of motion of solitary waves can be reverted by changing Γ.

In summary, the important effects of a dynamic motor distribution are (i) the appearance of a characteristic wave-length independent of the system size, (ii) the appearance of aster-like solutions, and (iii) that the existence of inhomogeneous states requires a symmetric situation with $c_0^+ = c_0^-$.

V. CONTRACTILE TENSION AND EXTERNAL FORCES

So far, we have been focusing on dynamical properties of active bundles. We now discuss mechanical properties of the bundle such as bundle tension and the role of applied external forces. The total tension $\Sigma(y)$ at a point y within the bundle is obtained by integrating the contributions of all filaments, i.e.,

$$\Sigma(y) = \int dx \left[\sigma^+(x, y) + \sigma^-(x, y) \right] \quad , \qquad (45)$$

where $\sigma^\pm(x, y)$ has been introduced in Eqs. (4) and (5). Taking into account momentum conservation, Eq. (6), one finds in the absence of external forces

$$\frac{d}{dy}\Sigma(y) = \int dx \left[f_{\mathrm{fl}}^+ + f_{\mathrm{fl}}^- + f_{\mathrm{m}}^+ + f_{\mathrm{m}}^- \right] \quad . \qquad (46)$$

This equation allows us to calculate the tension profile by means of Eq. (8) if the currents $J^\pm$ are known.

For simplicity, we neglect again f_{m}. The total tension in the bundle can be written as

$$\Sigma(y) = \Sigma_{\rightrightarrows}(y) + \Sigma_{\rightleftarrows}(y) \quad . \tag{47}$$

Here, we have introduced the tension due to interactions between filaments of the same orientation, $\Sigma_{\rightrightarrows}$, and those of opposite orientation, $\Sigma_{\rightleftarrows}$. From Eq. (46) we obtain

$$\Sigma_{\rightrightarrows}(y) = -\eta \int dx (J^{++}(x) + J^{--}(x)) Q(x-y) + \Sigma_{\rightrightarrows}^{(0)} \tag{48}$$

$$\Sigma_{\rightleftarrows}(y) = -\eta \int dx (J^{+-}(x) + J^{-+}(x)) Q(x-y) + \Sigma_{\rightleftarrows}^{(0)} \quad , \tag{49}$$

where $\frac{d}{dx}Q(x) = R(x)$ with $Q(0) = 0$, and $\Sigma_{\rightrightarrows}^{(0)}$ and $\Sigma_{\rightleftarrows}^{(0)}$ are constants of integration. These expressions seem to imply that the tension at position y depends on the global state of the bundle since $Q(x) \neq 0$ for all $x \neq 0$. However,

tension is a local quantity as can be seen by introducing the function $P(x,\xi) = Q(x+\xi) - Q(x)$. For the minimal model with $R(x) = 1$ for $|x| < \ell/2$ and $R(x) = 0$ otherwise we obtain

$$\Sigma_{\rightrightarrows}(y) = \frac{1}{2}\alpha\eta \int_{-\ell}^{\ell} d\xi \int dx \, c^+(x+\xi)c^+(x)P(x-y,\xi)\mathrm{sgn}(\xi)$$
$$+\frac{1}{2}\alpha\eta \int_{-\ell}^{\ell} d\xi \int dx \, c^-(x+\xi)c^-(x)P(x-y,\xi)\mathrm{sgn}(\xi) \tag{50}$$

and

$$\Sigma_{\rightleftarrows}(y) = \frac{1}{2}\beta\eta \int_{-\ell}^{\ell} d\xi \int dx \, c^-(x+\xi)c^+(x)P(x-y,\xi)$$
$$-\frac{1}{2}\beta\eta \int_{-\ell}^{\ell} d\xi \int dx \, c^+(x+\xi)c^-(x)P(x-y,\xi) \quad . \tag{51}$$

In contrast to the non-local function Q, P is a local function, with $P(x,\xi) = 0$ for $|x| > 2\ell$. In writing the above equations, we have dropped constant contributions to the tension arising from the boundaries. Indeed, if we consider a situation with periodic boundary conditions, such boundary terms must vanish. The integration constants $\Sigma_{\rightrightarrows}^{(0)}$ and $\Sigma_{\rightleftarrows}^{(0)}$ are therefore determined by the condition that in the final expressions (50) and (51) constant contributions to the tension are absent.

The tension in the homogeneous state $c^\pm(x) = c_0^\pm$, is given by

$$\Sigma = \frac{1}{2}\eta\ell^3\alpha(c_0^{+2} + c_0^{-2}) \quad . \tag{52}$$

In this case only the interaction between parallel filaments contributes to the active part of the bundle tension. For an oriented bundle, the tension is positive, i.e., contractile, whenever $\alpha > 0$.

More compact expressions can be obtained by the approximation $P(x,\xi) = \xi$ for $|x| < \ell/2$ and $P(x,\xi) = 0$ elsewhere. Then

$$\Sigma_{\rightrightarrows}(y) \approx \frac{1}{2}\alpha\eta \int_{y-\ell/2}^{y+\ell/2} dx \int_{-\ell}^{\ell} d\xi \, |\xi|(c^+(x+\xi)c^+(x) + c^-(x+\xi)c^-(x)) \tag{53}$$

and

$$\Sigma_{\rightleftarrows}(y) \approx \frac{1}{2}\beta\eta \int_{y-\ell/2}^{y+\ell/2} dx \int_{-\ell}^{\ell} d\xi\, \xi(c^+(x+\xi)c^-(x) - c^-(x+\xi)c^+(x)) \quad . \tag{54}$$

For filament distributions that vary weakly over a filament length, this result corresponds to the expressions given in Ref. [22], with $\bar{\eta} = \eta/2$ and $\tilde{\eta} = \eta/4$.

Contractile tension in the bundle can give rise to contractile forces exerted by the bundle. In order to illustrate this, consider a homogeneous oriented bundle with constant filament density $c(x) = c_0$ inside a box $0 \leq x \leq L$ of size L while $c(x) = 0$ elsewhere. In order to stabilize this state, we impose boundary conditions which immobilize filaments within the intervals $[0, \ell]$ and $[L - \ell, L]$ near the ends. Such boundary conditions could be realized by attaching the filaments near the end to a substrate. This filament distribution is stationary and for $\alpha < \alpha_c$ stable in the interval $[\ell, L - \ell]$. At the ends, the force balance Eq. (7) is satisfied only if the force density $f_{\text{ext}}(x) = \alpha\eta\ell c_0^2(\ell - x)$ is applied for $x \in [0, \ell]$ and correspondingly at the right end. The total force acting on the ends is thus $F = \int_0^{\ell} f_{\text{ext}}(x)dx = \Sigma$. This result indicates, that the generated force is independent of the bundle length and increases with the square of the filament density.

VI. DISCUSSION

In this paper, we have developed a physical description for the dynamics and mechanics of active filament bundles. In this one-dimensional description, we describe the dynamics of the filament densities projected on an axis which is parallel to the filaments. The activity in these bundles results from active cross-links, that create relative forces between the filaments. Our approach is based on momentum conservation within the bundle and momentum exchange via external forces. Dynamic equations can be derived most conveniently using simplifying assumptions such as a low motor density or low duty ratio, local friction, the absence of passive cross-linkers, and the assumption that filaments do not change their lengths. At low motor densities the filament currents are dominantly generated by interactions of filament pairs. Using this approach we systematically derive the minimal model introduced in earlier works. In general, the filament dynamics in the active bundle is described by nonlinear integro-differential equations. The nonlocal character of these equations reflect the finite filament length.

The bundle dynamics on scales much larger than the filament length alternatively can be described phenomenologically in a continuum limit, leading to a nonlinear description in the form of partial differential equations [30]. Such an approach is not limited by the above mentioned simplifying assumptions. However, the origin of the different terms which appear in the equations cannot be systematically related to more microscopic mechanisms. Interestingly, the main features found in phenomenological descriptions are already captured by the more specific models described here, which are derived using simple approximations. This suggests that the main features obtained from our models can still hold in situations where our approximations are no longer valid.

The equations discussed in this paper describe the average behavior of the bundle and thus represent a mean-field theory where fluctuations are captured by effective diffusion terms but do not explicitly appear in the description. In particular, the coefficient D of filament diffusion is effectively generated by motor-filament interactions. In the absence of such interactions, thermal fluctuations would lead to a diffusion coefficient $D \simeq kT/\eta\ell$, which becomes small for long filaments. The effective diffusion coefficient due to active interactions between parallel filaments, which do not generate a net current in the homogeneous state, can be estimated as $D \simeq \Delta x^2\omega$. Here Δx is the run-length of a motor on a filament and $\omega \sim \ell$ denotes the rate of generation of mobile cross-links, which grows linearly with the filament length. As a consequence, $D \sim \ell$ and for long filaments the diffusion is dominated by active cross-links. Numerical simulations of computer models, which take into account fluctuations show, that the phenomena described in the previous sections persist qualitatively in the presence of fluctuations [22]. A thorough analysis of the effect of fluctuations will be the subject of a separate publication [30].

The minimal model which neglects the dynamics of the motor distribution already exhibits a complex scenario of behaviors. We discuss the full bifurcation diagram of this model which involves homogeneous solutions, contracted steady states, solitary waves and oscillatory waves. These states are separated by bifurcations and can partly coexist depending on parameter values.

Taking into account the dynamics of the motor distribution does again generate the types of solutions present in the minimal model. Furthermore, new inhomogeneous steady states occur which are the one-dimensional analog of asters. In addition, the bifurcation diagrams are modified and are considerably richer. Contracted steady states are destabilized by the motor dynamics and in many cases become solitary waves. Furthermore, instabilities of the homogeneous state already occur in the absence of interactions between filaments of the same orientation, i.e. $A = 0$. The bifurcation diagrams exhibits for certain parameter ranges reentrant behavior, i.e. the homogeneous state is re-stabilized by increasing A or B.

External forces modify the filament dynamics in inter-

esting ways. Using the momentum balance in the filament bundle, we studied active mechanical properties of the bundle. In general, the bundle generates mechanical tension. Applying external forces to the bundle ends, a stationary state of a contractile bundle can be attained.

It is interesting to compare our results to experiments, where purified filaments interact with motor molecules or small aggregates of such motors. There is one in vitro experiment involving filament bundles [9], where the contraction accompanied by polarity sorting of disordered bundles of actin filaments in the presence of ATP and myosin II molecules (more specifically HMM), which presumably spontaneously form small aggregates, has been observed. Qualitatively, this corresponds to the state shown in Fig. 8. However, this experiment has not been repeated and a systematic in vitro study exploring all the regimes discussed in this paper is lacking and would be very valuable. Experiments on filament bundles could also be performed using microtubules, however, suitable preparations techniques to generate aligned filaments have to be developed. Artificially constructed kinesin aggregates would be natural candidates for mobile cross-links used in such a study.

As mentioned above, our results are expected to be more general and could also apply to situations where additional components are present. For example it may be more convenient to prepare filament bundles using the help of passive cross-linking or bundling proteins like α-actinin. For a large cross-linker density or a long lifetime of such passive cross-links we expect qualitatively new behaviors. However, for low concentrations or short lifetimes of passive cross-links they are expected to mainly modify the effective friction coefficient and possibly other parameters of our model. Even in the presence of passive cross-links, we expect the main results of our work to apply in certain regimes.

A similar modification of model parameters can be expected in general, if other proteins are present which interact with motors and/or filaments. For example, the interaction strength α between equally oriented filaments could be significantly enhanced by proteins bound to filaments which affect the speed of motors. In fact, it might seem odd at first glance that filaments of the same orientation exhibit significant interactions via motors at all. As a motor advances on both filaments with the same speed, no relative motion is generated. Interactions between filaments of the same orientation are induced by motors that do not move with the same speed on two cross-linked filaments. This happens, e.g., when a motor arrives on one filament at the end towards which it moves. In this case, the motor stops on one filament while continuing for a while to move on the second filament. This induces relative filament sliding via an end-effect.

The interaction strength α between equally oriented filaments can be enhanced if the motor speed varies along the whole filament. For example, the speed of motors can be affected by the presence of other motors on the same filament. Such crowding would typically lead to a slowing down of motors as they approach the filament end [34], generating relative motion of filament pairs. Furthermore, one could imagine specific proteins bound to the filaments which affect the speed of motors. If such proteins had a graded distribution linked to the filament polarity, they would lead to strong interaction terms between filaments of the same orientation. These examples illustrate, that in more complex situations where additional proteins are present, the main results of our work could still apply, however, with effective parameters.

This suggest, that the essential properties of active filament bundles found in our work might be even more general and could also apply to more complex situations found in vivo. For example, our results could apply to stress fibers. These are contractile actin bundles in cells lacking the obvious periodic organization of muscles [1] but containing myosins and other proteins. As we have demonstrated in Sect. V, the generation of tension and contraction is possible through the interaction of filament pairs without the need of a muscle-like sarcomere structure. The periodic boundary conditions which we use in several examples correspond to the situation, where the bundle forms a ring and could apply for example to contractile rings which cleaves a cell during cell division.

Interestingly, the types of dynamic behaviors which we observe also include qualitatively the symmetry breaking presented by fragments of fish keratocytes [16, 17]. These fragments consist of the lamellipodium, which is the flattened leading margin of these cells, responsible for their migration. Notably, they do contain neither the nucleus nor microtubules. These fragments exist in a symmetric stationary state as well as in an asymmetric locomoting state, where one can change between these states through sufficiently strong external perturbations [17]. Even though the active bundles studied in the present work are far from giving a description of moving keratocyte fragments, our results clearly indicate, that viewing the cytoskeleton as a dynamical system is a valuable concept for understanding such phenomena. Our description of active bundles provides a firm basis for the development of more profound theories of active filament systems, which could help understanding self-organization and dynamic behaviors in living cells such as cell locomotion. Moving on into this direction will require a number of important additional ingredients. A three dimensional description should, for example, incorporate effects, such as the polymerization and depolymerization of filaments, non-mobile cross-linkers, capping proteins, and the interaction of filaments with a membrane.

APPENDIX A: EIGENVALUES OF THE LINEARIZED TIME-EVOLUTION OPERATOR

Here, we give the complete eigenvalues of the linearized time-evolution operator $\Lambda(k)$ of the minimal model given in Eq. (29) and show, that $\alpha_c > 0$.

The two eigenvalues of $\Lambda(k)$ are

$$
\begin{aligned}
\lambda_\pm &= -k^2 + \alpha(1 - \cos k)c - 2i\beta k\delta c \\
&\pm \left\{ \alpha^2(1 - \cos k)^2\delta c^2 - \beta^2 k^2 c^2 + \beta^2 \sin^2 k(c^2 - \delta c^2) + 2i\alpha\beta k(1 - \cos k)c\delta c \right\}^{1/2} \quad . \tag{A1}
\end{aligned}
$$

In this expression $c = c_0^+ + c_0^-$ and $\delta c = c_0^+ - c_0^-$. The real part of λ_+, which determines the stability of the homogeneous state against small perturbations, is

$$
\lambda(k) = -k^2 + \alpha(1 - \cos k)c + \left\{ \frac{1}{2}\sqrt{a^2 + b^2} + \frac{1}{2}a \right\}^{1/2} \tag{A2}
$$

with

$$
\begin{aligned}
a &= \alpha^2(1 - \cos k)^2\delta c^2 \\
&\quad -\beta^2 k^2 c^2 + \beta^2 \sin^2 k(c^2 - \delta c^2) \tag{A3} \\
b &= 2\alpha\beta k(1 - \cos k)c\delta c \quad . \tag{A4}
\end{aligned}
$$

For $\alpha = 0$ this implies $\lambda(k) = -k^2$. The derivative of λ with respect to α is of the form

$$
\frac{\partial\lambda}{\partial\alpha} = A_0 + A_1\alpha + A_2\alpha^3 \tag{A5}
$$

with $A_i > 0$, $i = 0, 1, 2$. It then follows that there is a unique critical value $\alpha_c > 0$, determined by $\lambda(k = 2\pi/L; \alpha = \alpha_c) = 0$, such that the homogenous state is linearly stable unless $\alpha > \alpha_c$ and that the longest wavelength fitting in the system becomes unstable.

APPENDIX B: NON-HOMOGENEOUS SOLUTIONS CLOSE TO α_C

We calculate the asymptotic solutions of the minimal model close to the critical value α_c for arbitrary β and compare it to the expressions for small β discussed in sect. III.

1. Oriented bundles

In Fourier-representation the stationary solution of Eq. (21) is given by

$$
c_k = -\frac{2\alpha}{k}\sum_p \frac{\cos p - 1}{p}c_p c_{k-p} \quad , \tag{B1}
$$

where $c_{-k} = c_k^*$. In particular

$$
c_1 = -\frac{2\alpha L^2}{4\pi^2}\left\{ \left[\cos\frac{2\pi}{L} - 1\right]c_1 c_0 + \frac{1}{2}\left[\cos\frac{4\pi}{L} - 1\right]c_2 c_{-1} - \left[\cos\frac{2\pi}{L} - 1\right]c_{-1} c_2 + \ldots \right\} \tag{B2}
$$

$$
c_2 = -\frac{\alpha L^2}{4\pi^2}\left\{ \left[\cos\frac{2\pi}{L} - 1\right]c_1 c_1 + \frac{1}{2}\left[\cos\frac{4\pi}{L} - 1\right]c_2 c_0 + \ldots \right\} \tag{B3}
$$

Close to $\alpha = \alpha_c$, we expand the solution in terms of c_1 using the ansatz $c_k \propto c_1^k$. Ignoring higher modes, we obtain

$$
c_2 = -\frac{1}{1 + \frac{\alpha L^2}{4\pi^2}\frac{1}{2}\left[\cos\frac{4\pi}{L} - 1\right]c_0}\frac{\alpha L^2}{4\pi^2}\left[\cos\frac{2\pi}{L} - 1\right]c_1^2. \tag{B4}
$$

Up to third order in c_1 we find

$$
F(\alpha)c_1 - G(\alpha)|c_1|^2 c_1 = 0, \tag{B5}
$$

with

$$
F(\alpha) = 1 + \frac{2\alpha L^2}{4\pi^2}\left[\cos\frac{2\pi}{L} - 1\right]c_0 \tag{B6}
$$

and

$$G(\alpha) = \frac{2\alpha L^2}{4\pi^2} \left\{ \frac{1}{2} \left[\cos \frac{4\pi}{L} - 1 \right] - \left[\cos \frac{2\pi}{L} - 1 \right] \right\} \frac{\frac{\alpha L^2}{4\pi^2} \left[\cos \frac{2\pi}{L} - 1 \right]}{1 + \frac{\alpha L^2}{4\pi^2} \frac{1}{2} \left[\cos \frac{4\pi}{L} - 1 \right] c_0}. \tag{B7}$$

The Fourier coefficients of the stationary solution are given by

$$c_1 = \frac{Lc_0}{2\pi} \sqrt{\frac{-2c_0}{\cos \frac{2\pi}{L}}} \left[1 - \cos \frac{2\pi}{L} \right] (\alpha - \alpha_c)^{1/2} + O\left((\alpha - \alpha_c)^{3/2} \right) \tag{B8}$$

and

$$c_2 = -\frac{2L^2 c_0^2}{4\pi^2} \frac{1 - \cos \frac{2\pi}{L}}{\cos \frac{2\pi}{L}} (\alpha - \alpha_c) + O\left((\alpha - \alpha_c)^2 \right). \tag{B9}$$

2. Bundles of mixed orientation

We determine solitary waves which appear at the bifurcation point $\alpha = \alpha_c$ using the ansatz

$$c^{\pm}(x, t) = \sum c_k^{\pm} e^{ik(2\pi x/L + \omega t)}. \tag{B10}$$

The Fourier coefficients satisfy the following equations:

$$iwc_1^+ = -\frac{4\pi^2}{L^2} c_1^+ + 2\alpha \left\{ \left[1 - \cos \frac{2\pi}{L} \right] (c_1^+ c_0^+ - c_{-1}^+ c_2^+) + \frac{1}{2} \left[1 - \cos \frac{4\pi}{L} \right] c_{-1}^+ c_2^+ + \ldots \right\}$$
$$+ 2i\beta \left\{ \frac{2\pi}{L} c_0^- c_1^+ + \sin \frac{2\pi}{L} (c_1^- c_0^+ + c_{-1}^- c_2^+) + \frac{1}{2} \sin \frac{4\pi}{L} c_2^- c_{-1}^+ + \ldots \right\} \tag{B11}$$

$$2iwc_2^+ = -\frac{16\pi^2}{L^2} c_2^+ + 4\alpha \left\{ \left[1 - \cos \frac{2\pi}{L} \right] c_1^+ c_1^+ + \frac{1}{2} \left[1 - \cos \frac{4\pi}{L} \right] c_2^+ c_0^+ + \ldots \right\}$$
$$+ 4i\beta \left\{ \frac{2\pi}{L} c_0^- c_2^+ + \sin \frac{2\pi}{L} c_1^- c_1^+ + \frac{1}{2} \sin \frac{4\pi}{L} c_2^- c_0^+ + \ldots \right\} \tag{B12}$$

$$iwc_1^- = -\frac{4\pi^2}{L^2} c_1^- + 2\alpha \left\{ \left[1 - \cos \frac{2\pi}{L} \right] (c_1^- c_0^- - c_{-1}^- c_2^-) + \frac{1}{2} \left[1 - \cos \frac{4\pi}{L} \right] c_{-1}^- c_2^- + \ldots \right\}$$
$$- 2i\beta \left\{ \frac{2\pi}{L} c_0^+ c_1^- + \sin \frac{2\pi}{L} (c_1^+ c_0^- + c_{-1}^+ c_2^-) + \frac{1}{2} \sin \frac{4\pi}{L} c_2^+ c_{-1}^- + \ldots \right\} \tag{B13}$$

$$2iwc_2^- = -\frac{16\pi^2}{L^2} c_2^- + 4\alpha \left\{ \left[1 - \cos \frac{2\pi}{L} \right] c_1^- c_1^- + \frac{1}{2} \left[1 - \cos \frac{4\pi}{L} \right] c_2^- c_0^- + \ldots \right\}$$
$$- 4i\beta \left\{ \frac{2\pi}{L} c_0^+ c_2^- + \sin \frac{2\pi}{L} c_1^+ c_1^- + \frac{1}{2} \sin \frac{4\pi}{L} c_2^+ c_0^- \ldots \right\}. \tag{B14}$$

$$\vdots$$

We assume without loss of generality $c_0^+ > c_0^-$ and expand in c_1^+, which leads to

$$F(\alpha, \beta, \omega) - G(\alpha, \beta, \omega)|c_1^+|^2 = 0, \tag{B15}$$

where the expressions for F and G to first order in β are given by

$$F = -\frac{4\pi^2}{L^2} + 2\alpha \left[1 - \cos \frac{2\pi}{L} \right] c_0^+ + i \left[\frac{4\pi}{L} \beta c_0^- - \omega \right] \tag{B16}$$

and

$$G = 8\alpha^2 \frac{L^2}{4\pi^2} \left[1 - \cos \frac{2\pi}{L} \right] \left\{ \left[1 - \cos \frac{2\pi}{L} \right] - \frac{1}{2} \left[1 - \cos \frac{4\pi}{L} \right] \right\} \left\{ \frac{1}{\Delta} - 2i \frac{\omega_1 - \frac{4\pi^2}{L} c_0^-}{\Delta^2} \beta \right\} \qquad (B17)$$

Here, $\Delta = 16\pi^2/L^2 - 2\alpha \left[1 - \cos \frac{4\pi}{L} \right] c_0^+$.

At the bifurcation point $\alpha = \alpha_c$ we have $F(\alpha_c, \beta, \omega_0) = 0$. In first order in $\alpha - \alpha_c$ we obtain for the frequency and the amplitude of c_1^+

$$\omega = \omega_0 + \omega_1(\alpha - \alpha_c) + \dots \qquad (B18)$$

$$|c_1^+|^2 = \frac{\partial_\alpha F(\alpha_c, \omega_0) + \omega_1 \partial_\omega F(\alpha_c, \omega_0)}{G(\alpha_c, \omega_0)}(\alpha - \alpha_c) + \qquad (B19)$$

The right hand side of the last expression needs to be real and positive such that we obtain the condition

$$\text{Im} \frac{\partial_\alpha F(\alpha_c, \omega_0)}{G(\alpha_c, \omega_0)} = \omega_1 \text{Im} \frac{\partial_\omega F(\alpha_c, \omega_0)}{G(\alpha_c, \omega_0)}. \qquad (B20)$$

Furthermore, the sign of the prefactor of $\alpha - \alpha_c$ will determine if the bifurcation is super- oder sub-critical.

The bifurcation condition $F(\alpha_c, \omega_0) = 0$ leads to

$$\alpha_c = \frac{4\pi}{L^2} \frac{1}{2 \left[1 - \cos \frac{2\pi}{L} \right] c_0^+} \qquad (B21)$$

$$\omega_0 = \frac{4\pi}{L} \beta c_0^- \quad . \qquad (B22)$$

This implies

$$\partial_\alpha F(\alpha_c, \omega_0) = \frac{2L^2}{4\pi^2} \left[1 - \cos 2\pi L \right] c_0^+ \qquad (B23)$$

$$\partial_\omega F(\alpha_c, \omega_0) = -i \frac{L^2}{4\pi^2} \qquad (B24)$$

$$G(\alpha_c, \omega_0) = -\frac{1}{c_0^2 {}^2} \frac{\cos \frac{2\pi}{L}}{1 - \cos \frac{2\pi}{L}} \quad , \qquad (B25)$$

and $\omega_1 = 0$.

The velocity of propagation is given by $v = \omega_0 L/2\pi = 2\beta c_0^-$. The components c_1^+ and c_2^+ are given by the expressions (B8) and (B9) for c_1 and c_2, respectively. For the distribution of minus-filaments we find

$$c_1^- = -2i\beta \frac{\sin \frac{2\pi}{L} c_0^-}{\frac{4\pi^2}{L^2} - 2\alpha \left[1 - \cos \frac{2\pi}{L} \right] c_0^-} c_1^+ \qquad (B26)$$

$$c_2^- = i\beta \frac{\sin \frac{2\pi}{L} \left[1 - \cos \frac{2\pi}{L} \right]^2 c_0^{+2} c_0^-}{\frac{16\pi^4}{L^4} \left\{ 1 - \frac{1}{2} \left[1 + \cos \frac{2\pi}{L} \right] \frac{c_0^+ + c_0^-}{c_0^+} + \frac{1}{4} \left[1 + \cos \frac{2\pi}{L} \right]^2 \frac{c_0^-}{c_0^+} \right\}} (\alpha - \alpha_c) + O\left((\alpha - \alpha_c)^2 \right). \qquad (B27)$$

These expressions are consistent with the results of Sec. III B and provide analytic expressions of solitary wave solutions for small β.

APPENDIX C: FILAMENT-ADHESION

In this section, we discuss the effects on the bundle dynamics due to filament adhesion to a substrate in the minimal model. Adhering filaments are described by the densities a^+ and a^-, respectively. Attached filaments

are assumed to be immobile, while they contribute to the motion of free filaments. The dynamic equations in dimensionless form are given by

$$\partial_t c^+ = \partial_x^2 c^+ - \partial_x J^{++} - \partial_x J^{+-} - \omega_a c^+ + \omega_d a^+ \quad (C1)$$
$$\partial_t c^- = \partial_x^2 c^- - \partial_x J^{--} - \partial_x J^{-+} - \omega_a c^- + \omega_d a^- \quad (C2)$$
$$\partial_t a^+ = \omega_a c^+ - \omega_d a^+ \qquad (C3)$$
$$\partial_t a^- = \omega_a c^- - \omega_d a^- \qquad (C4)$$

with

$$J^{\pm\pm} = \int_0^1 d\xi \, \left[\alpha c^\pm(x + \xi) + \bar{\alpha} a^\pm(x + \xi) - \alpha c^\pm(x - \xi) - \bar{\alpha} a^\pm(x - \xi) \right] c^\pm(x) \qquad (C5)$$

and

$$J^{\pm\mp} = \mp \int_{-1}^{1} d\xi \; \left[\beta c^{\mp}(x+\xi) + \bar{\beta} a^{\mp}(x+\xi)\right] c^{\pm}(x) \quad . \tag{C6}$$
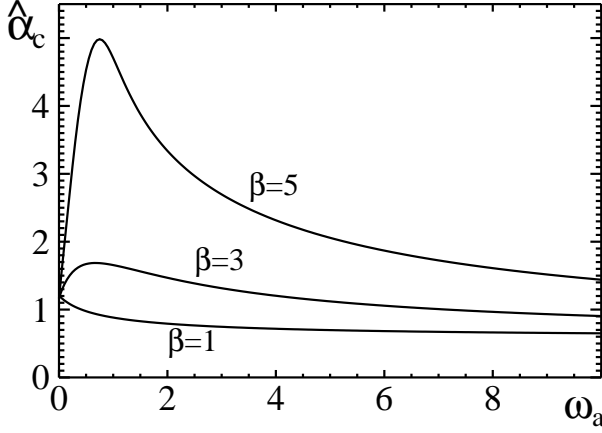

FIG. 9: The effect of filament adhesion on the critical value $\hat{\alpha}_c$ of the minimal model. Displayed is the critical value $\hat{\alpha}_c$ as a function of the adhesion rate ω_a for different values of the coupling strength β and for $c_0^+ = 0.3$, $c_0^- = 0.7$, $\bar{\alpha} = 2\alpha$, $\bar{\beta} = 2\beta$, $\omega_d = 1$, and $L = 10$. For $\omega_a = 0$ $\hat{\alpha}_c = \alpha_c$, which is the critical value in the minimal model in the absence of adhesion.

Here ω_a and ω_d are rates of attachment and detachment of filaments, respectively while $\bar{\alpha}$ and $\bar{\beta}$ characterize coupling constants between free and attached filaments.

The homogeneous state $c^{\pm}(x) = c_0^{\pm}$ and $a^{\pm}(x) = \omega_a c_0^{\pm}/\omega_d$ is stationary. It becomes unstable at a critical value α_c which for oriented bundles is given by

$$\hat{\alpha}_c = \alpha_c \frac{\omega_a + \omega_d}{\mu\omega_a + \omega_d}, \tag{C7}$$

where α_c is the critical value in the minimal model with $\omega_a = 0$ and for $\mu = \bar{\alpha}/\alpha$. For $\beta \neq 0$ a Hopf-bifurcation occurs, the dependence of the critical value $\hat{\alpha}_c$ on the attachment rate ω_a is shown in Fig. 9 for $\bar{\alpha} = 2\alpha$ and $\bar{\beta} = 2\beta$.

In the case $\beta = 0$, the stationary distributions are given by $c^{\pm}(x;\omega_a) = \frac{\omega_d}{\mu\omega_a+\omega_d}c^{\pm}(x;0)$ and $a^{\pm}(x;\omega_a) = \frac{\omega_a}{\mu\omega_a+\omega_d}c^{\pm}(x;0)$ where $c^{\pm}(x;0)$ denote the stationary states of the minimal model. For $\beta \neq 0$ solutions can be obtained in the limit of small attachment rates by expanding around solitary waves for $\omega_a = 0$. Consider a

solitary wave in the minimal model given by $c^{\pm}(x,t;0) = u_0^{\pm}(x - v_0 t)$ and $a^{\pm}(x,t;0) = 0$. Assuming that for finite ω_a solutions of the form $c^{\pm}(x,t;\omega_a) = u^{\pm}(x - vt)$ and
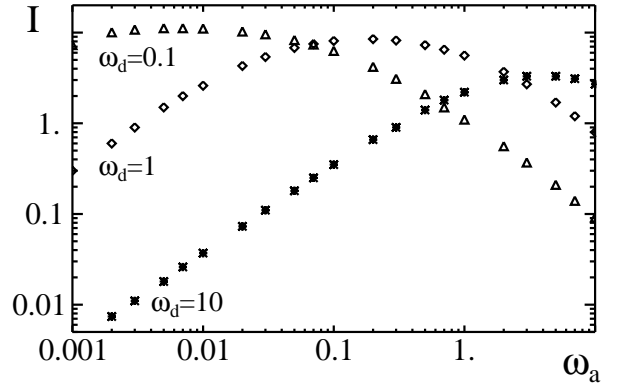

FIG. 10: The total filament current I of propagating filament patterns with filament adhesion as a function of the adhesion rate ω_a. Symbols represent numerically obtained results for different detachment rates ω_d. Parameters are $\alpha = 1.5$, $\beta = 2$, $\bar{\beta} = 2\beta$, $c_0^+ = 0.3$, $c_0^- = 0.7$, and $L = 10$. The maximal current decreases and is reached at larger ratios of ω_a/ω_d as ω_d is increased.

$a^{\pm}(x,t:\omega_a) = r^{\pm}(x - vt)$ exist, we write

$$v = v_0 + \omega_a v_1 + \ldots \tag{C8}$$
$$u^{\pm} = u_0^{\pm} + \omega_a u_1^{\pm} + \ldots \tag{C9}$$
$$r^{\pm} = \omega_a r_1^{\pm} + \ldots \tag{C10}$$

The equations for $r_1^{\pm}$ can be solved explicitly. We find

$$r_1^{\pm}(x) = \frac{1}{e^{\omega_d T} - 1} \int_0^T dt' \; e^{\omega_d t'} u_0^{\pm}(x - v_0 t') \quad , \tag{C11}$$

where $T = v_0 L$.

This result can in turn be used to calculate in first order in ω_a the total net current I associated with these solitary waves. Indeed, in lowest order this current is given by

$$I = 2\omega_a \int_0^L dx \left\{ \alpha \int_0^1 d\xi \left[\left(r_1^+(x+\xi) - r_1^+(x-\xi) \right) u_0^+(x) + \left(r_1^-(x+\xi) - r_1^-(x-\xi) \right) u_0^-(x) \right] \right.$$
$$\left. + \beta \int_{-1}^1 d\xi \left[r_1^+(x+\xi) u_0^-(x) - r_1^-(x+\xi) u_0^+(x) \right] \right\} \quad , \tag{C12}$$

where, for simplicity, we have chosen $\bar{\alpha} = 2\alpha$ and $\bar{\beta} = 2\beta$. Evaluating this expression using Eq. (C11) and $u_0^\pm(x) = \sum_{n=-\infty}^\infty u_{0,n}^\pm e^{i2\pi nx/L}$ we obtain

$$I = 8\omega_a L^3 v_0 \alpha \sum_{n=1}^\infty A_n \left(|u_{0,n}^+|^2 + |u_{0,n}^-|^2 \right) + O(\omega_a^2) \quad , \tag{C13}$$

where

$$A_n = \frac{\cos\frac{2\pi n}{L} - 1}{\omega_d^2 L^2 + 4\pi^2 n^2 v_0^2} \tag{C14}$$

with v_0 and $u_0^\pm$ depending on β as described in Sec. III B. This result shows, that solitary waves are accompanied with a net filament transport if filament adhesion occurs. Since $A_n < 0$ for all n, this transport occurs into the opposite direction as wave propagation. Remarkably, as indicated by the prefactor α, it is the interaction between *parallel* filaments that generates the current. Note, that for $\beta = 0$ we have $v_0 = 0$ and thus $I = 0$. Numerical results for I as a function of ω_a are shown in Fig. 10.

[1] B. Alberts, A. Johnson, J. Lewis, M. Raff, K. Roberts, and P. Walter, *Molecular biology of the cell* (Garland, New York, 2002), 4th ed.

[2] D. Bray, *Cell movements* (Garland, New York, 2001), 2nd ed.

[3] T. Kreis and R. Vale, *Cytoskeletal and motor proteins* (Oxford University Press, New York, 1993).

[4] F. Jülicher, A. Ajdari, and J. Prost, Rev. Mod. Phys. **69**, 1269 (1997).

[5] F. Amblard, A. C. Maggs, B. Yurke, A. N. Pargellis, and S. Leibler, Phys. Rev. Lett. **77**, 4470 (1996).

[6] F. C. MacKintosh and P. A. Janmey, Curr. Opin. Solid State & Mat. Sci. **2**, 350 (1997).

[7] D. C. Morse, Macromolecules **31**, 7030 (1998).

[8] L. LeGoff, F. Amblard, and E. M. Furst, Phys. Rev. Lett. **88**, 018101 (2002).

[9] K. Takiguchi, J. Biochem. **109**, 520 (1991).

[10] R. Urrutia, M. A. McNiven, J. P. Albanesi, D. B. Murphy, and B. Kachar, Proc. Natl. Acad. Sci. **88**, 6701 (1991).

[11] F. Nédélec, T. Surrey, A. C. Maggs, and S. Leibler, Nature **389**, 305 (1997).

[12] T. Surrey, M. B. Elowitz, P.-E. Wolf, F. Yang, F. Nédélec, K. Shokat, and S. Leibler, Proc. Natl. Acad. Sci. USA **95**, 4293 (1998).

[13] F. Nédélec and T. Surrey, C. R. Acad. Sci. Paris, Série IV **2**, 841 (2001).

[14] T. Surrey, F. Nédélec, S. Leibler, and E. Karsenti, Science **292**, 1167 (2001).

[15] A. A. Hyman and E. Karsenti, Cell **84**, 401 (1996).

[16] U. Euteneuer and M. Schliwa, Nature **310**, 58 (1984).

[17] A. B. Verkhovsky, T. M. Svitkina, and G. G. Borisy, Curr. Biol. **9**, 11 (1999).

[18] D. Humphrey, C. Duggan, D. Saha, D. Smith, and J. Käs, Nature **416**, 744 (2002).

[19] O. Thoumine and A. Ott, MRS Bull. **25**, 22 (1999).

[20] H. Nakazawa and K.Sekimoto, J. Phys. Soc. Jpn. **65**, 2404 (1996).

[21] K. Sekimoto and H. Nakazawa, in *Current topics in physics*, edited by Y. M. Cho, J. B. Hong, and C. N. Yang (World Scientific, Singapore, 1998), p. 394, physics/0004044.

[22] K. Kruse and F. Jülicher, Phys. Rev. Lett. **85**, 1778 (2000).

[23] K. Kruse, S. Camalet, and F. Jülicher, Phys. Rev. Lett. **87**, 138101 (2001).

[24] S. Camalet, F. Jülicher, and J. Prost, Phys. Rev. Lett. **82**, 1590 (1999).

[25] S. Camalet and F. Jülicher, New J. Phys. **2**, 24 (2000).

[26] B. Bassetti, M. C. Lagomarsino, and P. Jona, Eur. Phys. J. B **15**, 483 (2000).

[27] H. Y. Lee and M. Kardar, Phys. Rev. E **64**, 056113 (2001).

[28] T. B. Liverpool and M. C. Marchetti, cond-mat/0207320.

[29] T. B. Liverpool, A. C. Maggs, and A. Ajdari, Phys. Rev. Lett. **86**, 4171 (2001).

[30] K. Kruse and F. Jülicher, to be published.

[31] J. Howard, Nature **389**, 561 (1997).

[32] A. Ishijima, H. Kojima, H. Higuchi, Y. Harada, T. Funatsu, and T. Yanagida, Biophys. J. **70**, 383 (1996).

[33] F. Nédélec, T. Surrey, and A. C. Maggs, Phys. Rev. Lett. **86**, 3192 (2001).

[34] K. Kruse and K. Sekimoto, Phys. Rev. E **66**, 031904 (2002).